

Second Order Sliding Mode Observers for Fault Detection of Robot Manipulators

Daniele Brambilla, Luca M. Capisani, Antonella Ferrara, and Pierluigi Pisu

Abstract—The problem of detecting actuator and sensor faults of a robot manipulator using a model-based Fault Detection (FD) technique is addressed. With the proposed FD scheme it is possible to detect a single fault, which can occur on a specific actuator or on a specific sensor. The proposed scheme is composed by an Unknown Input Observer (UIO) and a modified Generalized Observer Scheme (GOS) to make analytical redundancy. The first enables the actuators FD, while the second enables the FD on the sensors. The Sub-Optimal Second Order Sliding Mode Control (SOSMC) approach is exploited to determine the input laws of the observers. The proposed approach is verified in simulation and experimentally on a COMAU SMART3-S2 robot manipulator.

I. INTRODUCTION

Any automatically controlled system is subject to the occurrence of faults. These faults can occur on each component of the plant in an unpredictable way, then it is fundamental to assure the capability of the diagnostic system to make possible a prompt detection of these events [1]–[3]. In this way, a reduction of the probability of mechanical damages or critical injuries to the people who operate around the controlled system can be achieved.

Faults can be modeled as an unexpected change of the dynamics of the system or as an unexpected presence of unknown signals affecting the components of the system. In a robot manipulator, a single fault can occur on a specific actuator, on a specific sensor or on a mechanical component of the system. The actuator and sensor faults are more frequent, because of the presence of electrical devices and electrical connections. Diagnostic systems are introduced to generate diagnostic signals which are useful to detect and isolate the fault presence. Residual generators are typically based on observers (see, for instance, [4]–[6]). However, noise and uncertainties can reduce the performances of the observers. Particular techniques are adopted in order to overcome these effects, such as linear filters [6]. An alternative efficient way to estimate input faults, in order to reduce noise and uncertainties, is the use of the so-called generalized momenta, see [7], [8].

Sliding mode based techniques are frequently adopted to accomplish the state observation [9]–[11]. Usually, the Fault Detection (FD) is possible by combining multiple sliding mode state observers [6], [12]–[14].

D. Brambilla, L. M. Capisani, and A. Ferrara are with Dept. of Computer Engineering and Systems Science, University of Pavia, 27100 Pavia, Italy danielle.brambilla02@ateneopv.it, {luca.capisani,antonella.ferrara}@unipv.it

P. Pisu is with the Department of Mechanical Engineering, Clemson University, Clemson, SC, USA pisup@clemson.edu

In this paper, a fault detection scheme is presented. It is based on an Unknown Input Observer (UIO) (see [10]) to detect and identify an actuator fault, and on a Generalized Observer Scheme (GOS) (see [5]) to detect a sensor fault. Robustness of the observers is enhanced by considering as input law of each observer a second order sliding mode law, in particular of *Sub-Optimal* type [15]. With this input law, a second order sliding manifold can be reached in finite time, in spite of the uncertainties. In this way the asymptotical convergence to zero of the observation errors is theoretically guaranteed. Because of the GOS structure, only a single sensor fault can be detected at a time. Sufficient conditions are given in order to make the fault isolation possible in particular working conditions.

Simulation and experimental results are presented in the paper. Simulations are based on the identified model of a COMAU SMART3-S2 robot manipulator, while experiments are made directly on this robot.

II. THE CONSIDERED FAULT SCENARIOS

In this paper, the case of a single fault occurring on the inputs or on the outputs of a robot manipulator is considered.

A. Actuator faults

In this situation, the real torque applied by the actuator is unknown. That is, $\tau \in \mathbb{R}^n$ being the nominal torque calculated by the robot controller, while $\Delta\tau \in \mathbb{R}^n$ being the input fault, the actual torque vector which is the input of the robotic system, can be expressed as $\bar{\tau}(t) = \tau(t) + \Delta\tau(t)$ (see Fig. 1). In practice, this fault can be caused by a damage that can occur on power supply systems, or actuator mechanisms, or wirings (but we will not distinguish among them).

B. Sensor faults

In this situation, the control system cannot determine the exact angular displacements of the joints. Let $q \in \mathbb{R}^n$ be the true but unknown output (i.e. the joints displacements), while $\Delta q \in \mathbb{R}^n$ be the vector of the fault signals acting on it. Then, $\bar{q} \in \mathbb{R}^n$ represents the value that the control system receives, i.e., $\bar{q}(t) = q(t) + \Delta q(t)$ (see Fig. 1).

III. THE MANIPULATOR MODEL

In absence of faults the dynamics of a n -joints robot manipulator can be written in the joint space, by using the Lagrangian approach, as

$$\tau = B(q)\ddot{q} + C(q, \dot{q})\dot{q} + g(q) + F_v\dot{q} = B(q)\ddot{q} + \delta(q, \dot{q}) \quad (1)$$

(see [16]) where $q \in \mathbb{R}^n$, $B(q) \in \mathbb{R}^{n \times n}$ is the inertia matrix, $C(q, \dot{q})\dot{q} \in \mathbb{R}^n$ represents centripetal and Coriolis torques,

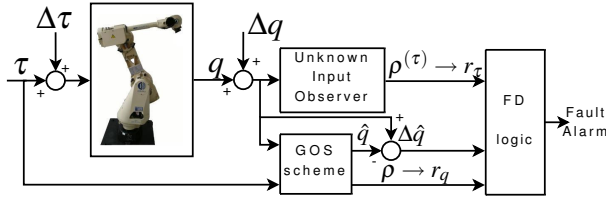


Fig. 1. The proposed FD scheme for actuator and sensor faults.

$F_v \in \mathbb{R}^{n \times n}$ is the viscous friction diagonal matrix, and $g(q) \in \mathbb{R}^n$ is the vector of gravitational torques. In this paper, it is assumed that the term $\delta(q, \dot{q})$ in (1) can be identified, while the term $B(q)$ is regarded as known. Then, the following relationship holds

$$\tau = B(q)\ddot{q} + \hat{\delta}(q, \dot{q}) + \eta = \hat{\tau} + \eta, \quad \eta = \delta - \hat{\delta} \quad (2)$$

where η is uncertain. Yet by virtue of the particular application considered, η can be assumed to be bounded.

IV. THE PROPOSED DIAGNOSTIC SCHEME

A. Actuators fault detection strategy

By relying on the so-called UIO approach [10], efficient estimators of the input torques can be designed [3], [17]. We propose to detect the actuator faults by means of an UIO of sliding mode type. The UIO hereafter described is a single multi-input-multi-state second order sliding mode observer, i.e.,

$$\begin{cases} \dot{\hat{\chi}}_1^{(\tau)} = \hat{\chi}_2^{(\tau)} \\ \dot{\hat{\chi}}_2^{(\tau)} = \hat{f}(\hat{\chi}_1^{(\tau)}, \hat{\chi}_2^{(\tau)}, \tau) + \rho^{(\tau)} \end{cases} \quad (3)$$

where $\hat{\chi}^{(\tau)} = [\hat{\chi}_1^{(\tau)}, \hat{\chi}_2^{(\tau)}]^T$ is the observer state, with $\hat{\chi}_1^{(\tau)} \in \mathbb{R}^n$, $\hat{\chi}_2^{(\tau)} \in \mathbb{R}^n$, and $f(\cdot)$ is defined as

$$\hat{f}(\cdot) = B^{-1}(\hat{\chi}_1^{(\tau)})[\tau - \hat{C}(\hat{\chi}_1^{(\tau)}, \hat{\chi}_2^{(\tau)})\hat{\chi}_2^{(\tau)} - \hat{F}_v\hat{\chi}_2^{(\tau)} - \hat{g}(\hat{\chi}_1^{(\tau)})] \quad (4)$$

where $\rho^{(\tau)}$ is the observer input law, it is determined as

$$\begin{cases} \dot{\rho}_i^{(\tau)}(t) = \alpha_i W_{iMAX} \text{sign} \left\{ s_i^{(\tau)}(t) - 0.5s_{iMAX}^{(\tau)} \right\} \\ \tilde{\chi}_1^{(\tau)} = q(t) - \hat{\chi}_1^{(\tau)}, \quad \tilde{\chi}_2^{(\tau)} = \dot{\tilde{\chi}}_1^{(\tau)} \\ s_i^{(\tau)}(t) = \tilde{\chi}_{2i}^{(\tau)} + \beta \tilde{\chi}_{1i}^{(\tau)} \end{cases} \quad (5)$$

that is, according to the so-called Sub-Optimal approach [15]. In (5), $s_i^{(\tau)}(t)$ is the so-called sliding variable, that is the variable to steer to zero in order to perform the observation task, i is the index of the component of the state vector coinciding with the actuator number, $s_{iMAX}^{(\tau)}$ represents the last extremal value of the sliding variable $s_i^{(\tau)}(t)$, and $\beta > 0$. It can be proved that a suitable choice of $\alpha_i W_{iMAX}$ exists such that the Sub-Optimal input law guarantees the exponential stability of the tracking error of this observer (the proof of this claim can be developed as in [15]).

Note that in case of input fault the dynamics of the robotic system given by (1) can be expressed as

$$\ddot{q} = f(q, \dot{q}, \tau + \Delta\tau) \quad (6)$$

The exponential stability of the observation error, implies that $\tilde{\chi}_1^{(\tau)} \rightarrow 0$, i.e.

$$\left[f(q, \dot{q}, \tau + \Delta\tau) - \hat{f}(\hat{\chi}_1^{(\tau)}, \hat{\chi}_2^{(\tau)}, \tau) - \rho^{(\tau)} \right] \rightarrow 0 \quad (7)$$

By virtue of the structure of the inverse model (1), it is apparent that an actuator fault $\Delta\tau$ can be modeled as a signal Δy acting at the acceleration level of the model, with $\Delta\tau = B(q)\Delta y$, because of the existence of the matrix $B^{-1}(q)$, $\forall q \in \mathbb{R}^n$. Then, (7) can be rewritten as

$$\begin{cases} \{ B(q)^{-1}[\tau - \delta(\cdot)] + \Delta y \\ -B^{-1}(\hat{\chi}_1)[\tau - \hat{\delta}(\cdot)] - \rho^{(\tau)} \} \rightarrow 0 \end{cases} \quad (8)$$

which implies the exponential convergence of $\rho^{(\tau)}$ to $\Delta y - B^{-1}(q)\eta$. Since the $B^{-1}(q)\eta$ term is bounded, suitable thresholds can be defined in order to enable the actuator fault detection. Note that, because of the fact that we assume that the modeling error η exists (which is quite realistic, as confirmed by the experimental tests), only faults exceeding the pre-specified thresholds can be detected, in contrast to the ideal case in which η is assumed to be zero and $\rho^{(\tau)} \rightarrow \Delta y$, so that any fault is detectable. Thresholds are selected as to minimize the probability of misdetection and false alarms, on the basis of experimental tests.

B. Sensors fault detection strategy: a GOS scheme with sliding mode observers

To perform the detection of sensor faults, n observers are used, one for each sensor. This strategy, called Generalized Observer Scheme (GOS) [5], and the proposed particular implementation are described in this section. The input law of the i^{th} GOS observer is calculated relying on all the sensor measurements, apart from the measurement coming from the i^{th} sensor (see Fig. 2). That is, the input law of the i^{th} GOS observer has the i^{th} component equal to zero.

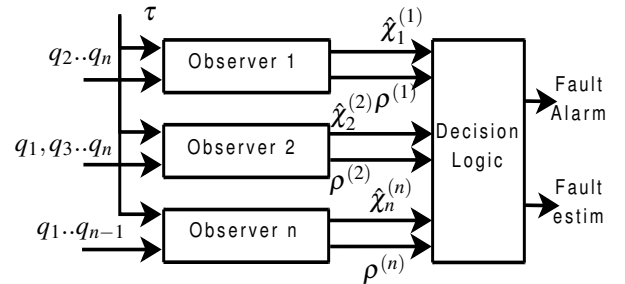


Fig. 2. Generalized Observer Scheme (GOS) for a n sensors system.

In the sequel, the following notation is considered for the vectors used in the GOS observers: $\hat{\chi}_1^{(i)} \in \mathbb{R}^n$ is the vector of the estimate of the \bar{q} vector made by the i^{th} observer, $e^{(i)} \in \mathbb{R}^n$ contains the corresponding observation errors, while $\rho^{(i)} \in \mathbb{R}^n$ is the input law of observer i . Moreover, the components of $\hat{\chi}_1^{(i)}$ are

$$\hat{\chi}_1^{(i)} = \left[\hat{\chi}_{1,1}^{(i)} \quad \hat{\chi}_{1,2}^{(i)} \quad \dots \quad \hat{\chi}_{1,n}^{(i)} \right]^T, \quad i = 1, \dots, n \quad (9)$$

Now, the i^{th} GOS observer in our proposal is defined as

$$\begin{cases} \dot{\hat{\chi}}_1^{(i)} = \hat{\chi}_2^{(i)} \\ \dot{\hat{\chi}}_2^{(i)} = \hat{f}(\hat{\chi}_1^{(i)}, \hat{\chi}_2^{(i)}, \tau) + \rho^{(i)}(t) \end{cases} \quad (10)$$

where $\hat{f}(\cdot)$ has the structure indicated in (4). Note that the form of the observer is quite obvious, taking into account the type of application and it is analogous to that adopted in [18] in the general case of mechanical systems. Moreover, in contrast to the actuator FD, for which a single observer is used, for sensor FD, n sliding mode observers are designed.

The considered error vector signal for the i^{th} observer is given by

$$e^{(i)} = q + \Delta q - \hat{\chi}_1^{(i)} \quad (11)$$

Then, also in this case, we design the observer input law $\rho^{(i)}(t)$ in (10) according to the Sub-Optimal Algorithm [15], by, in addition, posing the i^{th} component of $\rho^{(i)}(t)$ equal to zero, i.e.,

$$\begin{cases} \dot{\rho}_j^{(i)} = \alpha_j W_{jMAX} \text{sign} \{s_j^{(i)}(t) - 0.5s_{jMAX}^{(i)}\}, j \neq i \\ \rho_i^{(i)} = 0 \\ s^{(i)}(t) = \dot{e}^{(i)} + \beta e^{(i)} \end{cases} \quad (12)$$

In (12), $s^{(i)}(t)$ is the so-called sliding variable, that is the variable to steer to zero in order to perform the observation task, j is the index of the component of the state vector coinciding with the sensor number, $s_{jMAX}^{(i)}$ represents the last extremal value of the sliding variable $s_j^{(i)}(t)$, and $\beta > 0$. It can be proved that a suitable choice of $\alpha_j W_{jMAX}$ exists such that the Sub-Optimal input law guarantees the exponential stability of the tracking error of this observer (the proof of this claim can be developed as in [15]). Note that, with this input law, the observer (10) has the i^{th} component in open loop. This can imply stability problems also in absence of faults, if the system is not open loop stable by itself. However, this component of the i^{th} observer is just that useful, in case of fault on the i^{th} sensor, in order to give an estimate of the fault signal. To circumvent stability problems while avoiding to significantly alterate the detection, in the experimental tests, a local small gain proportional feedback is closed to generate the i^{th} input law component of the i^{th} observer (12). That is,

$$\rho_i^{(i)}(t) = K \left(q_i + \Delta q_i - \hat{\chi}_{1,i}^{(i)} \right), \forall i, K > 0 \quad (13)$$

with K small.

More precisely, if $\hat{f}(\cdot)$ can be assumed to be a quite accurate estimate of $f(\cdot)$, a fault can be detected considering Table I. As it can be seen from this table, when a single sensor fault occurs, only $n - 1$ of the n GOS observers have their input laws, i.e. $\rho^{(i)}$, sensitive to the fault, since the observer j , associated with the sensor where the fault has occurred, has the j^{th} component of the input law, i.e. $\rho_j^{(j)}$, always set equal to zero. During the robot operation, one can observe the n vectors $\rho^{(i)}$. If the situation is that depicted in a generic column of Table I, say the j^{th} , then one can conclude that the fault has occurred on sensor j . If,

in contrast, $\hat{f}(\cdot)$ differs from $f(\cdot)$ of the bounded quantity $B^{-1}(q)\eta$, as mentioned in Subsection IV-A, again thresholds need to be introduced to perform the fault detection. For instance, the entries of Table I expressed as $\rho^{(i)} \neq 0$ can be replaced by the condition

$$\text{if } \exists k \text{ s.t. } \left[\text{sign} \left\{ \rho^{(i)} \right\} \odot \rho^{(i)} \right]_k > T_k \quad (14)$$

while the entries of Table I expressed as $\rho^{(i)} = 0$ become

$$\left[\text{sign} \left\{ \rho^{(i)} \right\} \odot \rho^{(i)} \right]_k < T_k, \forall k = 1, \dots, n \quad (15)$$

where $\text{sign} \left\{ \rho^{(i)} \right\}$ is the vector containing the sign of each component of $\rho^{(i)}$, the symbol \odot denotes the Schur product, $[\cdot]_k$ denotes the k^{th} component of a vector, and T_k is a positive real number representing the selected threshold. As in the case addressed in Subsection IV-A, the values of the thresholds depend on the magnitude of the uncertain term $B^{-1}(q)\eta$. Obviously, now the fact that a fault has occurred on sensor j can be inferred when (15) is true for $i = j$ and (14) is true $\forall i \neq j$.

Sen. 1 fault $r_{q1} = 1$	Sen. 2 fault $r_{q2} = 1$...	Sen. n fault $r_{qn} = 1$
$\rho^{(1)} = 0$	$\rho^{(1)} \neq 0$...	$\rho^{(1)} \neq 0$
$\rho^{(2)} \neq 0$	$\rho^{(2)} = 0$...	$\rho^{(2)} \neq 0$
\vdots	\vdots	\vdots	\vdots
$\rho^{(n)} \neq 0$	$\rho^{(n)} \neq 0$...	$\rho^{(n)} = 0$

TABLE I

SIGNATURE TABLE FOR SENSOR FAULT ISOLATION.

C. Residual generation

Fig. 1 shows the complete diagnostic scheme for robot manipulators.

For implementation purposes, all the proposed algorithms are converted in discrete time. To deal with measurement noise in experiments, the following 5th order low-pass filter is introduced (z is the unitary delay operator)

$$\mathcal{F}(z) = \frac{b}{1 - az^{-1} - az^{-2} - az^{-3} - az^{-4} - az^{-5}} \quad (16)$$

with $a = 0.1993$ and $b = 1 - 5a$. The residual vector r_τ is given by

$$r_{\tau i} = \begin{cases} 0 & \text{if } |\mathcal{F}(t) * \rho_i^\tau| < T_i^\tau \\ 1 & \text{if } |\mathcal{F}(t) * \rho_i^\tau| > T_i^\tau \end{cases} \quad \forall i \quad (17)$$

while the residual vector r_q is obtained by filtering the $\rho_{j \neq i}^{(i)}(t)$ signals through the filter (16) and comparing these signals with their thresholds T_k , according to Table I. Thresholds T_i^τ and T_k take in account the presence of uncertainties and discrete time sampling. To choose suitable thresholds, some tuning experiments have to be executed.

D. The error signature table

To isolate a fault means to determine if the fault has occurred on a specific actuator or on a specific sensor.

The isolation of a fault can be performed by comparing the binary detection vector $[r_\tau, r_q]$ with the subsequent fault

Fault	$r_{\tau 1}$	$r_{\tau 2}$	$r_{\tau n}$	$r_{q 1}$	$r_{q 2}$	$r_{q n}$
None	0	0	0	0	0	0
Act. 1	1	0	0	p	p	p
Act. 2	0	1	0	p	p	p
Act. n	0	0	1	p	p	p
Sen. 1	p	p	p	1	0	0
Sen. 2	p	p	p	0	1	0
Sen. n	p	p	p	0	0	1

TABLE II

FAULT SIGNATURE TABLE, WHERE p REPRESENTS A VALUE THAT CAN BE 0 OR 1.

signature Table II. Note that in general, an actuator fault produces relevant residuals on all the n sensor fault observers and a sensor fault produces, in general, relevant residuals for the actuators. However, for a small fault on sensors, i.e., for small Δq , for small velocities and accelerations of the robot manipulator system, and in the absence of uncertainties, the actuator residual signal r_{τ} is not sensitive to a sensor fault Δq if $|B(q + \Delta q)\ddot{q} - B(q)\ddot{q} + \delta(q + \Delta q, \dot{q} + \Delta \dot{q}) - \delta(q, \dot{q})|$ is less than the actuator fault threshold.

The p values in Table II, take in account this fact, and, in general, a single fault cannot be exactly isolated if the fault induces the detection of one actuator fault and one sensor fault. From a theoretical point of view, it can be demonstrated that, in case of exact identification of the manipulator model, and in particular work conditions, a fault can be correctly isolated.

Theorem IV.1. *Under the assumptions of single fault, of exact knowledge of the manipulator model and the absence of noise on sensor measurements, a sensor fault Δq can be isolated from an actuator fault if the following conditions hold*

- the n degree of freedom manipulator belongs to a vertical plane, and each link has a non null gravitational contribution on each actuator;
- the sensor fault signal Δq is time invariant, i.e. $\Delta \dot{q} = \Delta \ddot{q} = 0$;
- the robot manipulator represented by the model (1) is in static work conditions, i.e. $\dot{q} = \ddot{q} = 0$.

In particular, when a single fault occurs on a specified component of the vector q , the former conditions assure that it is impossible to detect a non-existent single fault on $\Delta \tau$, (which represents a false alarm situation).

Remark 1. Note that the conditions stated in Theorem IV.1 can appear a little restrictive, but these conditions are only sufficient. In practice, a fault can be isolated in several situations, especially when $|\dot{q}|$ and $|\ddot{q}|$ are small.

V. A CASE STUDY

A. The considered manipulator

The fault detection technique described in this paper has been experimentally verified on a COMAU SMART3-S2 anthropomorphic rigid robot manipulator which is a classical example of industrial manipulator (see Fig. 3). It consists of six links and six rotational joints driven by brushless electric motors. For the sake of simplicity during the experiments the robot has been constrained to move on a vertical plane.

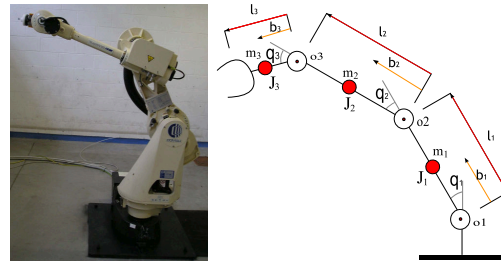


Fig. 3. The SMART3-S2 robot and the three link planar manipulator.

Then, it is possible to consider the robot as a three link-three joint, in the sequel numbered as $\{1, 2, 3\}$, planar manipulator (see Fig. 3). Yet, the method proposed in this paper holds for n -joints robots even of spatial type.

The controller has a sampling time of 0.001s, a 12 bit D/A and a 16 bit A/D converters. The joints positions are acquired by resolvers, fastened on the three motors, holding mechanical reducers with ratio $\{207, 60, 37\}$ respectively, while the maximum torques are $\{1825, 528, 71\}$ [Nm].

B. Parameters identification

The adopted identification procedure is based on the Maximum Likelihood (ML) approach as explained in [19] (in the absence of faults). To perform the identification, the dynamical model (1) can be written in the following form

$$Y = \Phi(q, \dot{q}, \ddot{q})\theta^o + V \quad (18)$$

where the nonlinear matrix function $\Phi(\cdot) \in \mathbb{R}^{3N \times 9}$ represents the model (1) in a parametrized linear form, N being the number of sampled data, and 3 being the number of the considered joints. The term $\theta^o = [\gamma_1 \dots \gamma_9]^T$, $\gamma_i \in \mathbb{R}$, represents the unknown parameter vector to be estimated, while $Y \in \mathbb{R}^{3N}$ is the torque applied by the actuators, and $V \in \mathbb{R}^{3N}$ is the noise acting on Y , which is the input of the robotic system. The parametrization of θ^o is shown in Table III, see [19], while in Table IV the values of the identified parameters for the considered robot are reported (expressed in SI units).

Parameter	Meaning
γ_1	$m_3 b_3^2 + J_3$
γ_2	$J_3 + m_3(l_2^2 + b_3^2) + J_2 + m_2 b_2^2$
γ_3	$J_3 + m_3(l_1^2 + l_2^2 + b_3^2) + J_2 + m_2(l_1^2 + b_2^2) + J_1 + m_1 b_1^2$
γ_4	$m_1 b_1 + m_2 l_1 + m_3 l_1$
γ_5, γ_6	$m_2 b_2 + m_3 l_2, m_3 b_3$
$\gamma_7, \gamma_8, \gamma_9$	F_{v1}, F_{v2}, F_{v3}

TABLE III

PARAMETRIZATION OF THE MANIPULATOR MODEL.

θ^{ML}	γ_1	γ_2	γ_3	γ_4	γ_5
$E[\theta^{ML}]$	0.297	10.07	87.91	57.03	9.21
$Var[\theta^{ML}]$	0.003	0.04	0.2	0.06	0.02
$\bar{\theta}^{ML}$	γ_6	γ_7	γ_8	γ_9	
$E[\theta^{ML}]$	0.316	66.3	14.71	8.29	
$Var[\theta^{ML}]$	0.003	0.3	0.1	0.02	

TABLE IV

AVERAGE VALUE AND VARIANCE FOR THE ESTIMATED PARAMETERS.

C. The manipulator control algorithm

To carry on the experiments on the COMAU SMART3-S2 manipulator it is necessary to control the robot. A particular control scheme is considered in this work, which consists of an inverse dynamics control performing a non ideal feedback linearization, combined with a robust second order sliding mode controller of Sub-Optimal type [15]. The application of this control scheme to a COMAU SMART3-S2 manipulator has already been described in [20].

VI. SIMULATION RESULTS

In the next two subsections, the performances of the proposed FD scheme for planar robot manipulators are verified, first by simulating an actuator fault, then by simulating a sensor fault. Note that noise is added on the input and output signals, in order to make the simulations be more realistic. Moreover, in simulation, the local small gain loop on the i^{th} component of the i^{th} observer of the GOS structure is not necessary because of the absence of unmodeled effects which can induce instability. This allows one to use the i^{th} component of the vector $\chi_1^{(i)}$ to identify the fault, so that our proposal in simulation can be regarded as a Fault Detection and Identification (FDI) scheme.

A. Actuators FDI

To simulate an actuator fault, we can consider the presence of an abrupt fault on joint 3: as one can see from Fig. 4 the fault amplitude is correctly identified.

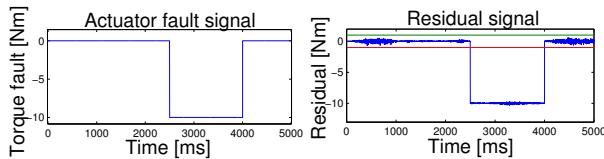


Fig. 4. FDI simulations on the third actuator.

B. Sensors FDI

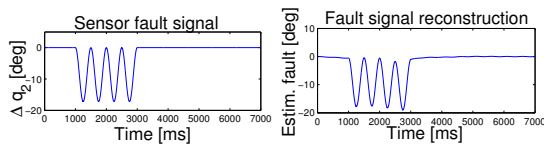


Fig. 5. Sensor FDI simulations: Δq_2 and $e_2^{(2)}$ signals in (10) in case of a fault acting on sensor 2.

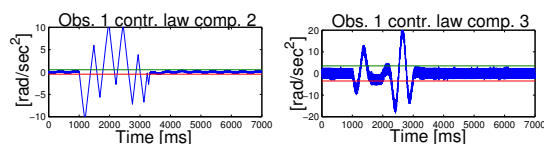


Fig. 6. Sensor FDI simulations: $\rho_2^{(1)}$ and $\rho_3^{(1)}$ signals in (10) in case of a fault on sensor 2.

A simulation of the presence of a single sinusoidal sensor fault on the second joint sensor is presented in this subsection. This fault is sporadic: it appears at time instant 1s, and disappears at time instant 3s. The identification of the fault

signal is illustrated in Fig. 5. It is based on the comparison of the estimated angular position and the measured angular position by the second joint sensor.

Figs. 6, 7, and 8 show the two components of the input laws of the three GOS observers which are not null (the third component is clearly equal to zero, as imposed by (12)). In particular, the fault isolation can be done considering the first and the third observer signals, while, as expected, the input law of the second observer is not affected by the fault. Note that some high frequency noise has been added to the input torque signals, and that fixed thresholds has been defined to detect the fault.

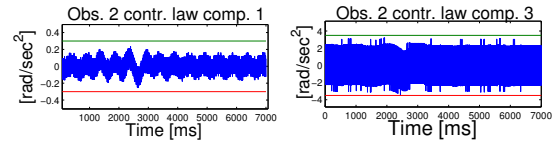


Fig. 7. Sensor FDI simulations: $\rho_1^{(2)}$ and $\rho_3^{(2)}$ signals in (10) in case of a fault on sensor 2.

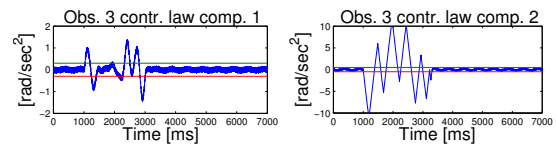


Fig. 8. Sensor FDI simulations: $\rho_1^{(3)}$ and $\rho_2^{(3)}$ signals in (10) in case of a fault on sensor 2.

VII. EXPERIMENTAL RESULTS

In this section the proposed scheme is experimentally tested on the COMAU SMART3-S2 manipulator. The faults presence is introduced in the control system by adding a fault signal to the control variable (in case of actuator fault) or to the sensor signal (in case of sensor fault).

In this case, noise and unmodeled nonlinear effects are naturally present then the sensor FD turns out to be critical.

A. Experimental FD of actuators

Some experiments dealing with actuator faults have been developed through the introduction of abrupt faults on each joint. To show the properties of the proposed scheme, a 10[Nm] fault signal on the third actuator is considered. Note that this fault is below the 20% of the maximum torque allowed by the corresponding actuator. As it can be seen from Fig. 9, the fault is correctly identified.

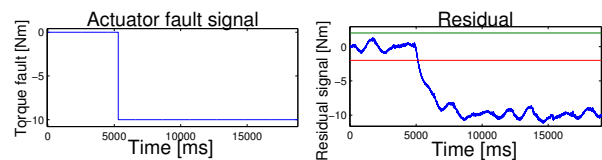


Fig. 9. FD experiment on the third actuator ($\Delta \tau$ and $(\hat{\tau} - \tau)$ signals).

B. Experimental FD of sensors

In the experimental case, the presence of nonlinear and unmodeled effects leads to a corruption of the signals useful for the fault analysis. The modified input law (13) for the GOS observers has been considered in this case.

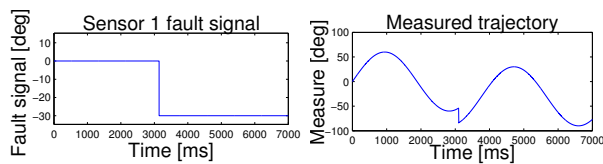


Fig. 10. Sensor FD experiment: q_1 and Δq_1 signals for a fault on sensor 1.

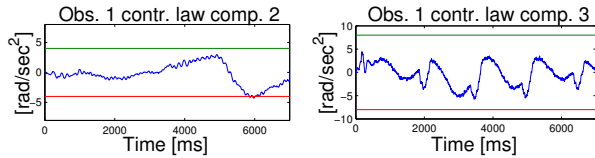


Fig. 11. Sensor FD experiments: $\rho_2^{(1)}$ and $\rho_3^{(1)}$ signals in (10) for a fault on sensor 1.

Relying on the modified structure, the following experiment is performed: an abrupt fault of $-30[\text{deg}]$ on the first joint sensor measurement is introduced starting from time instant 3.1s. In order to identify the joint on which the fault has occurred, the proposed fault signature table (Table II) is considered. Figs. 11, 12, and 13 show the two components different from zero of the input laws of the three GOS observers. The fault isolation can be accomplished considering the second and the third observer signals since only these (in particular one of their components) exceed the thresholds. So, one can conclude that the fault has occurred on sensor 1.

VIII. CONCLUSIONS

A FD scheme for robot manipulators based on the generation of second order sliding modes has been presented and has been experimentally tested on a COMAU SMART3-S2 robot manipulator, demonstrating good performances in detecting and identifying possible faults on the actuators, and in detecting the fault presence on a specific sensor. Note that the theoretical development presented in this paper allows one to deal with the following cases: faults (even multiple) occurring only on the actuators; single faults occurring on the actuators or on the sensors (the knowledge of the type of the device affected by the fault can be non available). Yet, in practical experiments we have observed that the identification of multiple sensor faults is possible, provided that they are not simultaneous.

REFERENCES

- [1] P. Pisu and G. Rizzoni, "A framework for model-based fault diagnosis with application to vehicle systems," in *Proc. 2nd IFAC Conference on Mechatronic Systems*, Berkeley, California, USA, Dec. 2002.
- [2] P. Pisu, A. Serrani, S. You, and L. Jalics, "Adaptive threshold based diagnostics for steer-by-wire systems," *ASME Transactions on Dynamics Systems, Measurement and Control*, vol. 128, no. 2, pp. 428–435, Jun. 2006.
- [3] C. De Persis and A. Isidori, "A geometric approach to nonlinear fault detection and isolation," *IEEE Transactions on Automatic Control*, vol. 46, no. 6, pp. 853–865, Jun. 2001.
- [4] W. Dixon, I. D. Walker, D. Dawson, and J. Hartfrant, "Fault detection for robot manipulators with parametric uncertainty: A prediction-error-based approach," *IEEE Transactions on Robotics and Automation*, vol. 16, no. 6, pp. 689–699, Dec. 2000.

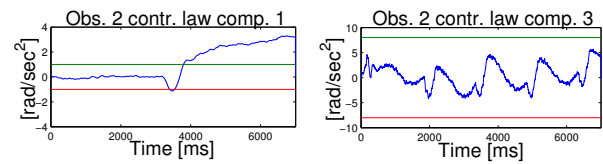


Fig. 12. Sensor FD experiments: $\rho_1^{(2)}$ and $\rho_3^{(2)}$ signals in (10) for a fault on sensor 1.

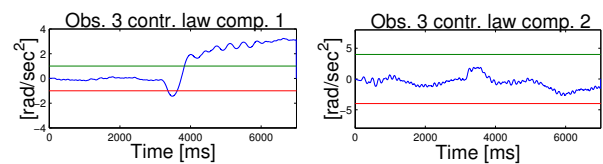


Fig. 13. Sensor FD experiments: $\rho_1^{(3)}$ and $\rho_2^{(3)}$ signals in (10) for a fault on sensor 1.

- [5] P. M. Frank, "Fault diagnosis in dynamic systems via state estimation – a survey," in *System fault diagnostics, reliability and related knowledge-based approaches*, Tzafestas, Singh, and Schmidt, Eds. Dort, Holland: Reidel Press, 1987, pp. 35–98.
- [6] C. Edwards, S. K. Spurgeon, and R. J. Patton, "Sliding mode observers for fault detection and isolation," *Automatica*, vol. 36, no. 4, pp. 541–553, Apr. 2000.
- [7] A. De Luca and R. Mattone, "Actuator failure detection and isolation using generalized momenta," in *Proc. IEEE International Conference on Robotics and Automation*, vol. 1, Taipei, Taiwan, Sep. 2003, pp. 634–639.
- [8] —, "An identification scheme for robot actuator faults," in *Proc. IEEE/RSJ International Conference on Intelligent Robots and Systems*, Alberta, Canada, Aug. 2005, pp. 1127–1131.
- [9] P. Pisu and A. Ferrara, "An observer-based second order sliding mode vehicle control strategy," in *Proc. IEEE 4th Intelligent Vehicles Symposium*, Dearborn, Michigan, USA, Oct. 2000, pp. 180–185.
- [10] C. Edwards, S. K. Spurgeon, and R. G. Hebden, "On development and applications of sliding mode observers," in *Variable Structure Systems: Toward XXIst Century, Lecture Notes on Control and Information Science*, J. Xu and Y. Xu, Eds. Berlin, Germany: Springer-Verlag, 2002, pp. 253–282.
- [11] F. J. J. Hermans and M. B. Zarrop, "Sliding mode observers for robust sensor monitoring," in *Proc. 13th IFAC World Congress*, San Francisco, California, USA, Jul. 1997, pp. 211–216.
- [12] C. P. Tan and C. Edwards, "Sliding mode observers for detection and reconstruction of sensor faults," *Automatica*, vol. 38, no. 10, pp. 1815–1821, Oct. 2002.
- [13] R. Sreedhar, B. Fernández, and G. Y. Masada, "Robust fault detection in nonlinear systems using sliding mode observers," in *Proc. IEEE Conference on Control Applications*, vol. 2, Vancouver, British Columbia, Canada, Sep. 1993, pp. 715–721.
- [14] W. Chen and M. Saif, "Robust fault detection and isolation in constrained nonlinear systems via a second order sliding mode observer," in *Proc. 15th IFAC World Congress*, Barcelona, Spain, Jul. 2002, pp. 1498–1500.
- [15] G. Bartolini, A. Ferrara, and E. Usai, "Chattering avoidance by second order sliding mode control," *IEEE Transactions on Automatic Control*, vol. 43, no. 2, pp. 241–246, Feb. 1998.
- [16] L. Sciacivico and B. Siciliano, *Modelling and Control of Robot Manipulators*, 2nd ed. London, UK: Springer-Verlag, 2000.
- [17] R. Mattone and A. De Luca, "Fault detection and isolation in mechanical systems," Department of Computer and System Science, University of La Sapienza, Rome, Italy, Tech. Rep., May 2004.
- [18] J. Davila, L. Fridman, and A. Levant, "Second-order sliding mode observer for mechanical systems," *IEEE Transactions on Automatic Control*, vol. 50, no. 11, pp. 1785–1789, Nov. 2005.
- [19] L. M. Capisani, A. Ferrara, and L. Magnani, "MIMO identification with optimal experiment design for rigid robot manipulators," in *Proc. IEEE/ASME International Conference on Advanced Intelligent Mechatronics*, Zürich, Switzerland, Sep. 2007, pp. 1–6.
- [20] —, "Design and experimental validation of a second order sliding-mode motion controller for robot manipulators," *International Journal of Control*, to appear, 2007.